Circulating Cell-Free DNA to Guide Prostate Cancer Treatment with PARP Inhibition

Jane Goodall[1], Joaquin Mateo[1,2], Wei Yuan[1], Helen Mossop[1], Nuria Porta[1], Susana Miranda[1], Raquel Perez-Lopez[1,2], David Dolling[1], Dan R. Robinson[3], Shahneen Sandhu[4], Gemma Fowler[1], Berni Ebbs[1], Penny Flohr[1], George Seed[1], Daniel Nava Rodrigues[1,2], Gunther Boysen[1], Claudia Bertan[1], Mark Atkin[1], Matthew Clarke[1], Mateus Crespo[1], Ines Figueiredo[1], Ruth Riisnaes[1], Semini Sumanasuriya[1,2], Pasquale Rescigno[1,2], Zafeiris Zafeiriou[1,2], Adam Sharp[1,2], Nina Tunariu[1,2], Diletta Bianchini[1,2], Alexa Gillman[1], Christopher J. Lord[1], Emma Hall[1], Arul M. Chinnaiyan[3], Suzanne Carreira[1], and Johann S. de Bono[1,2] for the TOPARP-A investigators

ABSTRACT

Biomarkers for more precise patient care are needed in metastatic prostate cancer. We have reported a phase II trial (TOPARP-A) of the PARP inhibitor olaparib in metastatic prostate cancer, demonstrating antitumor activity associating with homologous recombination DNA repair defects. We now report targeted and whole-exome sequencing of serial circulating cell-free DNA (cfDNA) samples collected during this trial. Decreases in cfDNA concentration independently associated with outcome in multivariable analyses (HR for overall survival at week 8: 0.19; 95% CI, 0.06–0.56; $P = 0.003$). All tumor tissue somatic DNA repair mutations were detectable in cfDNA; allele frequency of somatic mutations decreased selectively in responding patients (χ^2 $P < 0.001$). At disease progression, following response to olaparib, multiple subclonal aberrations reverting germline and somatic DNA repair mutations (*BRCA2, PALB2*) back in frame emerged as mechanisms of resistance. These data support the role of liquid biopsies as a predictive, prognostic, response, and resistance biomarker in metastatic prostate cancer.

SIGNIFICANCE: We report prospectively planned, serial, cfDNA analyses from patients with metastatic prostate cancer treated on an investigator-initiated phase II trial of olaparib. These analyses provide predictive, prognostic, response, and resistance data with "second hit" mutations first detectable at disease progression, suggesting clonal evolution from treatment-selective pressure and platinum resistance. *Cancer Discov; 7(9); 1006–17. ©2017 AACR.*

See related commentary by Domchek, p. 937.
See related article by Kondrashova et al., p. 984.
See related article by Quigley et al., p. 999.

[1]The Institute of Cancer Research, London, United Kingdom. [2]The Royal Marsden NHS Foundation Trust, London, United Kingdom. [3]The University of Michigan, Ann Arbor, Michigan. [4]Peter MacCallum Cancer Centre, Melbourne, Australia.

Note: Supplementary data for this article are available at Cancer Discovery Online (http://cancerdiscovery.aacrjournals.org/).

J. Goodall and J. Mateo contributed equally and are co-first authors of this article.

S. Carreira and J.S. de Bono are co-senior authors of this article.

Corresponding Author: Johann S. de Bono, The Institute of Cancer Research, The Royal Marsden NHS Foundation Trust, London SM2 5NG, United Kingdom. Phone: 44-20-8722-4028; Fax: 44-20-8642-7979; E-mail: johann.de-bono@icr.ac.uk

doi: 10.1158/2159-8290.CD-17-0261

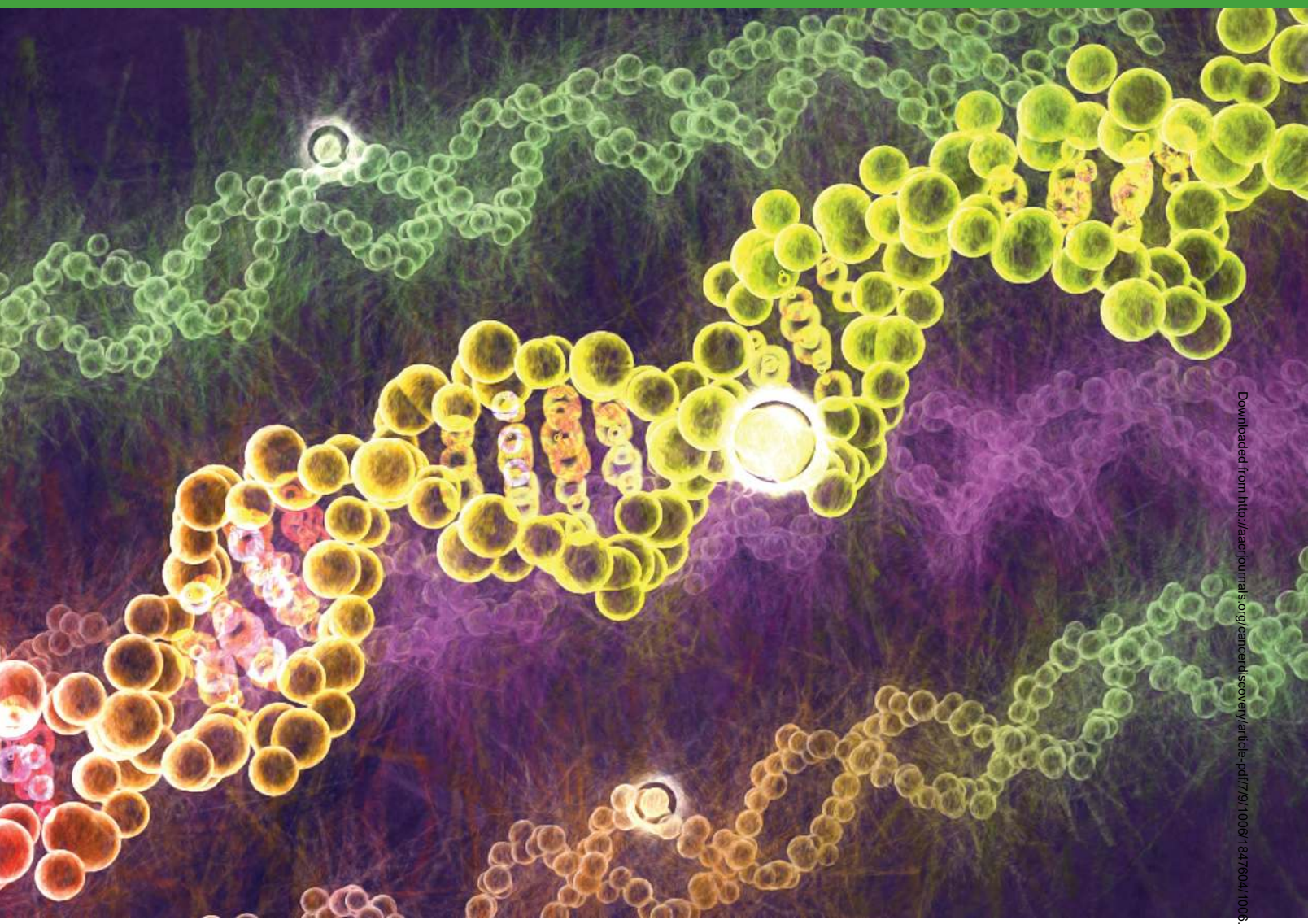

INTRODUCTION

Metastatic prostate cancer is a major cause of cancer mortality in males globally. Studies indicate substantial inter- and intrapatient genomic heterogeneity, although treatment to date has not incorporated molecular stratification (1–7). Clinical qualification of predictive biomarkers is a major need for these invariably lethal tumors. We previously reported that 20% to 30% of lethal prostate cancers have deleterious aberrations in genes involved in DNA repair by homologous recombination [homologous recombination deficiency (HRD)], including *BRCA2, ATM, BRCA1, PALB2, FANCA, CHEK2*, and *CDK12* (4). Studies indicate that HRD-associated mutations associate with a worse prognosis, with these aberrations being inherited in approximately 10% to 12% of men with lethal prostate cancer (8, 9).

We also recently reported an investigator-initiated phase II clinical trial (TOPARP-A) of the PARP inhibitor olaparib (Lynparza) in patients with metastatic prostate cancer, describing antitumor activity associating with HRD (10). These data led to olaparib being given "Breakthrough Designation" by the FDA for advanced prostate cancer associated with *BRCA2/ATM* defects, and registration trials of different PARP inhibitors being currently pursued (11–13). A major regulatory approval challenge for these drug development efforts remains the lack of proven surrogates of survival benefit. We hypothesized that circulating biomarkers can enhance drug development and patient care, informing on treatment response and resistance. Response biomarkers are crucial to improving the care of advanced prostate cancer, which is often characterized by metastatic disease only to bone, which is not easily evaluable (14). Circulating cell-free DNA (cfDNA) in blood, acquired from plasma by a simple blood test, provides repeated serial access to tumor DNA as a minimally invasive "liquid biopsy" (15–19).

We report here preplanned cfDNA analyses from serial blood samples from the TOPARP-A trial. We had hypothesized that cfDNA analyses can enhance drug development and patient care and that: (i) changes in cfDNA concentrations in response to treatment would be prognostic;

(ii) next-generation sequencing of cfDNA would detect the predictive HRD-associated mutations found in tumor biopsies; (iii) changes in cfDNA somatic mutation allele frequency on therapy would associate with response; and (iv) serial cfDNA analyses could detect the evolution of resistant subclones at disease progression.

RESULTS

Patient Characteristics and Blood Sample Disposition

Fifty patients were treated in the TOPARP-A trial; 49 were evaluable for response, with 16 patients responding to treatment. Overall, 16 of these 49 patients had prostate cancers with a deleterious aberration in homologous recombination DNA repair genes, with 14 of these patients responding to treatment. Serial samples for cfDNA studies were available for 46 of 49 patients (94%). We now report on these analyses utilizing updated outcome data based on a data snapshot taken on May 24, 2016. One patient with a *BRCA2* homozygous deletion remained on therapy and free of progression at the data cutoff, after 22 months of therapy. Overall, the median cfDNA baseline concentration across the trial population was 31.6 ng/mL [interquartile range (IQR), 19.4–57.1]. Next-generation targeted sequencing of cfDNA was successful for 43 of 46 patients (93%; Supplementary Fig. S1).

Prognostic Relevance of Changes in cfDNA Concentration Following PARP Inhibition

Changes in cfDNA concentration were evaluated in patients responding ($n = 16$) or not responding ($n = 30$) to olaparib. After 4 weeks of therapy, there was a median −51.4% change in responders (IQR, −72.6% to −29.5%) and a median −33.4% change in nonresponders (IQR, −52.3% to +5.5%; $P = 0.07$). After 8 weeks of therapy, responders continued to experience sustained declines (median −49.6% change; IQR, −76.5% to −20.4%), differing significantly from nonresponders (median +2.1% increase; IQR, −43.6% to +57.8%; $P = 0.006$; Supplementary Fig. S2).

Next, we explored how declines in cfDNA concentrations correlated with patient outcome based on radiologic progression-free survival (rPFS) and overall survival (OS). cfDNA concentration falls robustly correlated with rPFS as early as after 4 weeks of therapy [HR, 1.70; 95% confidence interval (CI), 1.13–2.55; $P = 0.01$ for cfDNA log fold change; HR, 0.41; 95% CI, 0.21–0.80; $P = 0.009$ for absence/presence of ≥50% fall from baseline of cfDNA concentration]. cfDNA concentration falls after 8 weeks of olaparib correlated with both prolonged rPFS and OS (Fig. 1).

In multivariable analyses including established prognostic factors, such as LDH and circulating tumor cell (CTC) count conversions, a ≥50% decline in cfDNA concentration after 4 weeks of olaparib was independently associated with longer rPFS. These changes at 4 weeks were not statistically significant for OS (HR, 0.47; 95% CI, 0.18–1.07; $P = 0.07$). Nevertheless, a ≥50% fall in cfDNA concentration after 8 weeks of therapy was independently associated with longer OS (HR for ≥50% cfDNA decline and OS in multivariable analyses: 0.19; 95% CI, 0.06–0.56; $P = 0.003$; Table 1).

Changes in Allele Frequency of Somatic Mutations

We then performed next-generation targeted sequencing of serial cfDNA samples to assess allele frequency of somatic mutations during PARP inhibitor therapy as an indirect estimate of tumor burden. A total of 254 plasma samples were analyzed. We detected somatic mutations in cfDNA of 33 of 43 baseline samples. Olaparib treatment led to sustained decreases in cfDNA mutation allele frequencies in responding patients; sustained (≥8 weeks) falls in cfDNA somatic mutation allele frequencies were not observed in nonresponding patients, although 3 of 29 detected somatic events in nonresponding patients decreased transiently after 4 weeks of olaparib (χ^2 $P < 0.001$; Fig. 2A).

Somatic HRD-Associated Mutations in cfDNA

Overall, 6 subjects in the TOPARP-A trial had tumors with somatic mutations likely to be associated with HRD (3 in *ATM*, 2 in *BRCA2*, 1 in *PALB2*; 5/6 responded to olaparib); all 6 mutations were detected in baseline cfDNA. In all 5 responding patients, these somatic mutation allele frequencies all decreased to <5% following olaparib treatment (Fig. 2B). In the nonresponding patient, the somatic mutation allele frequency remained unchanged at 4% throughout therapy.

In addition, in one nonresponding patient we detected two *ATM* frameshift mutations in cfDNA not previously detected in the tumor biopsy. Retrospective inspection of tumor data detected both mutations in 3% of sequencing reads. We obtained a further metastatic biopsy from a different anatomic location after treatment; both of these *ATM* mutations were present in 18% and 29% of reads, respectively. We also evaluated this patient's primary prostate tumor biopsy taken at diagnosis; one of these mutations was not present and the other was visualized in 1% of reads. Overall, these data indicate that these were probably subclonal mutations.

Loss of Heterozygosity in Germline Mutation Carriers

Five patients with pathogenic *BRCA2* or *ATM* germline mutations responded to olaparib in the trial. In 4 of these, we had previously documented loss of heterozygosity (LOH) for these pathogenic mutations in tumor biopsies. In these 4 patients, falls in the cfDNA allele frequencies of these germline mutations toward 50% were observed as they responded to olaparib, suggesting elimination of the tumor clone with LOH. For the last patient with an *ATM* mutation, but no LOH in his tumor biopsy, allele frequencies remained between 45% and 55% in the cfDNA at all time points in concordance with the tumor tissue findings (Fig. 2C).

Mechanisms of PARP Inhibitor Resistance Detected in cfDNA

Ten of 16 patients having an initial tumor response to olaparib had cfDNA samples acquired at the time of resistance and disease progression. In addition to targeted sequencing, we successfully performed whole-exome sequencing (WES) from paired plasma samples collected before olaparib treatment and at disease progression for 6 patients to study mechanisms of secondary resistance to PARP inhibition. In a seventh case, we performed WES in the progression sample

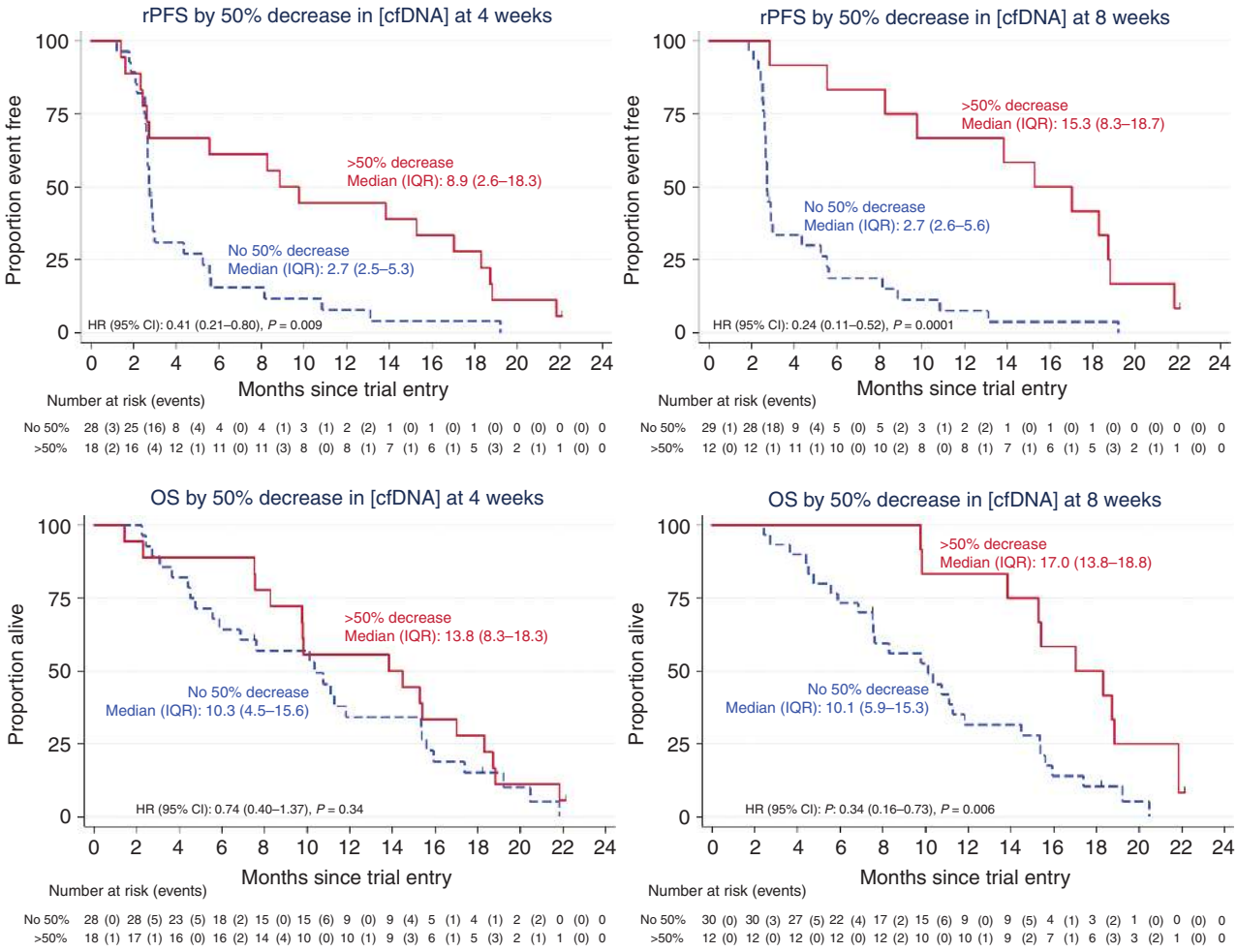

Figure 1. Kaplan–Meier plots showing differences in rPFS and OS based on the presence or absence of a ≥50% fall in total cfDNA concentration after 4 weeks and after 8 weeks of therapy with olaparib.

and targeted sequencing in the baseline cfDNA sample, due to low DNA yield.

In both of the patients with a germline *BRCA2* frameshift mutation, we identified at the time of tumor progression additional somatic *BRCA2* mutations in cfDNA restoring the normal open reading frame (Fig. 3).

One of these patients had a germline *BRCA2* p.-1056fs mutation and LOH in the pretrial tumor biopsy. At the time of disease progression, a further somatic deletion of four base pairs emerged, resulting in an overall in-frame change of four amino acids (p.K1057_Q1063delinsTEQA). In parallel, three other events were detected in different positions in the same genomic region, all of them also restoring the *BRCA2* normal open reading frame, and probably representing the coexistence of several resistant tumor subclones in cfDNA. This patient had bone metastases in the spine and pelvis; after an initial partial response to olaparib, he developed a heterogeneous pattern of progression after 9 months; a bone marrow biopsy of a relapse focused in the right hemipelvis was performed (Fig. 4). In this tumor sample, only one of the three emerging somatic reversions (p.K1057_Q1063delinsTEQA) was detected; these data suggest these other emerging subclones may have originated in different metastases.

A second germline *BRCA2* mutation carrier (p.E1514fs*15) developed an additional deletion of 28 bp at progression, reverting *BRCA2* back in frame. We confirmed the emergence of this new event independently by targeted next-generation sequencing (MiSeq). In addition, we also detected the emergence at progression of a somatic *ARID1A* mutation (p.Q1145*). These aberrations again indicate possible divergent clonal evolutionary resistance mechanisms as a result of PARP inhibition–generated selective pressures.

In nongermline mutation carriers, we also identified new emerging genomic events at progression leading to the reversion of a somatic *BRCA2* mutation (Fig. 5). A somatic 2-bp frameshift deletion was detected in WES of the original tumor biopsy and in targeted sequencing of the baseline plasma sample (p.Y2154fs*21). Because of DNA yield, we could not obtain WES of the baseline cfDNA sample in this patient. At progression, WES revealed two alternative deletions resulting in an in-frame deletion but restoring the open

Table 1. Univariate and multivariable Cox regression analyses of the association cfDNA plasma concentrations (ng/mL) with patient outcome including established prognostic factors.

		rPFS		OS	
Univariate analyses	***N***	**HR (95% CI)**	***P***	**HR (95% CI)**	***P***
4 weeks					
CTC conversion	47	0.30 (0.14–0.65)	0.002	0.53 (0.27–1.04)	0.07
≥30% CTC decline	47	0.33 (0.15–0.74)	0.007	0.86 (0.42–1.74)	0.67
cfDNA [c] log-fold change	46	1.70 (1.13–2.55)	0.01	1.30 (0.87–1.95)	0.19
≥30% cfDNA [c] decline	46	0.61 (0.33–1.14)	0.12	0.70 (0.37–1.32)	0.27
≥50% cfDNA [c] decline	46	0.41 (0.21–0.80)	0.009	0.74 (0.40–1.37)	0.34
8 weeks					
CTC conversion	41	0.38 (0.19–0.74)	0.005[a]	0.74 (0.39–1.42)	0.37[a]
≥30% CTC decline	41	0.61 (0.31–1.19)	0.15	1.21 (0.62–2.37)	0.58
cfDNA [c] log-fold change	42	1.83 (1.22–2.74)	0.003	1.43 (0.98–2.09)	0.06
≥30% cfDNA [c] decline	42	0.48 (0.25–0.92)	0.028	0.66 (0.34–1.26)	0.20
≥50% cfDNA [c] decline	42	0.24 (0.11–0.52)	0.0001	0.34 (0.16–0.73)	0.006
Multivariate analyses		**HR (95% CI)**	***P***	**HR (95% CI)**	***P***
4 weeks					
LDH		1.00 (1.00–1.00)	0.058	1.00 (1.00–1.00)	0.012
ECOG status 2 (vs. 0–1)		1.48 (0.50–4.38)	0.48	1.74 (0.60–5.06)	0.31
Radiological progression at trial entry (vs. PSA progression only)		1.01 (0.42–2.43)	0.98	0.20 (0.07–0.52)	0.001
Measurable disease at trial entry		0.32 (0.13–0.79)	0.014	0.50 (0.20–1.29)	0.154
Baseline CTC		1.00 (0.99–1.00)	0.20	1.00 (1.00–1.00)	0.34
Baseline cfDNA		1.00 (1.00–1.01)	0.54	1.00 (1.00–1.01)	0.23
CTC conversion		0.19 (0.07–0.05)	0.001	0.41 (0.17–1.01)	0.051
≥50% cfDNA [c] decline		0.25 (0.09–0.66)	0.005	0.44 (0.18–1.07)	0.071
8 weeks					
LDH		1.00 (1.00–1.01)	0.036	1.00 (1.00–1.01)	<0.001
ECOG status 2 (vs. 0–1)		2.45 (0.73–8.24)	0.15	2.55 (0.81–7.98)	0.11
Radiologic progression at trial entry (vs. PSA progression only)		1.37 (0.47–4.00)	0.57	0.24 (0.08–0.72)	0.011
Measurable disease at trial entry		0.49 (0.18–1.31)	0.15	0.53 (0.19–1.50)	0.24
Baseline CTC		1.00 (1.00–1.00)	0.83	1.00 (0.99–1.00)	0.24
Baseline cfDNA		1.00 (0.99–1.00)	0.32	1.00 (0.99–1.01)	0.89
CTC conversion		0.10 (0.03–0.28)	<0.001	0.35 (0.15–0.85)	0.020
≥50% cfDNA [c] decline		0.09 (0.03–0.30)	<0.001	0.19 (0.06–0.56)	0.003

Abbreviations: ECOG, Eastern Cooperative Oncology Group; LDH, lactate dehydrogenase.
[a]Indicates when proportional hazards assumption is not met.

reading frame of *BRCA2* coexisting with the original clone containing the frameshift mutation.

In addition, secondary genomic events causing reversion back to normal reading frame of a somatic *PALB2* mutation were also detected for one patient. The pretreatment sample contained a 2-bp frameshift deletion (p.-253fs*3) with LOH. At the time of progression, after 9 months of treatment, two different new mutations restoring the *PALB2* reading frame were identified (Fig. 5). Both events coexisted with the original clone, again indicating divergent resistant subclones.

We examined the nucleotide sequences flanking the *BRCA2* and *PALB2* original frameshift deletions in these cases with

Figure 2. **A,** Waterfall plot summarizing change in allele frequency (AF; defined as allele frequency on treatment subtracted by the allele frequency at baseline *100) after 4- and 8 weeks of therapy. Stars, patients considered responders to olaparib in the TOPARP-A trial in the predefined primary endpoint. An absolute decrease of ≥10% in allele frequency was observed in 18 of 27 somatic mutations detected in responding patients as compared with 3 of 29 somatic events monitored in nonresponding patients (χ^2 $P < 0.001$). None of the three allele frequency falls in nonresponding patients were maintained after 8 weeks of therapy. **B,** Four examples of how AF of somatic HRD-associated mutations decrease in response to therapy, in parallel with decreases in total cfDNA concentrations. A patient with an ATM p.-2288fs mutation had intermittent increases and decreases in AF in parallel to drug interruptions due to hematologic toxicity. **C,** Changes in cfDNA mutation allele frequency over time in germline deleterious mutation carriers (*BRCA2* and *ATM*) in 5 patients from the TOPARP-A trial. Those patients with LOH at baseline have the cfDNA mutation allele frequency trending toward 50% in response to therapy, probably due to elimination of the tumor clone. This is not seen in the serial cfDNA samples from the patient whose tumor did not have LOH.

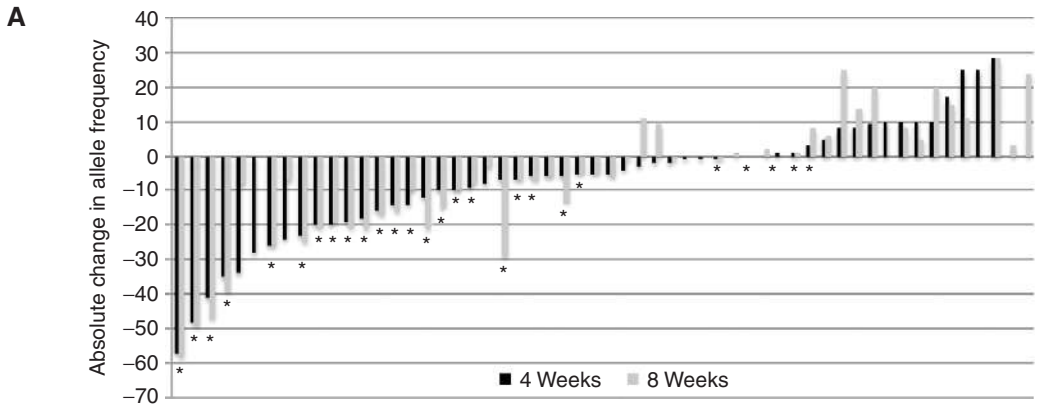

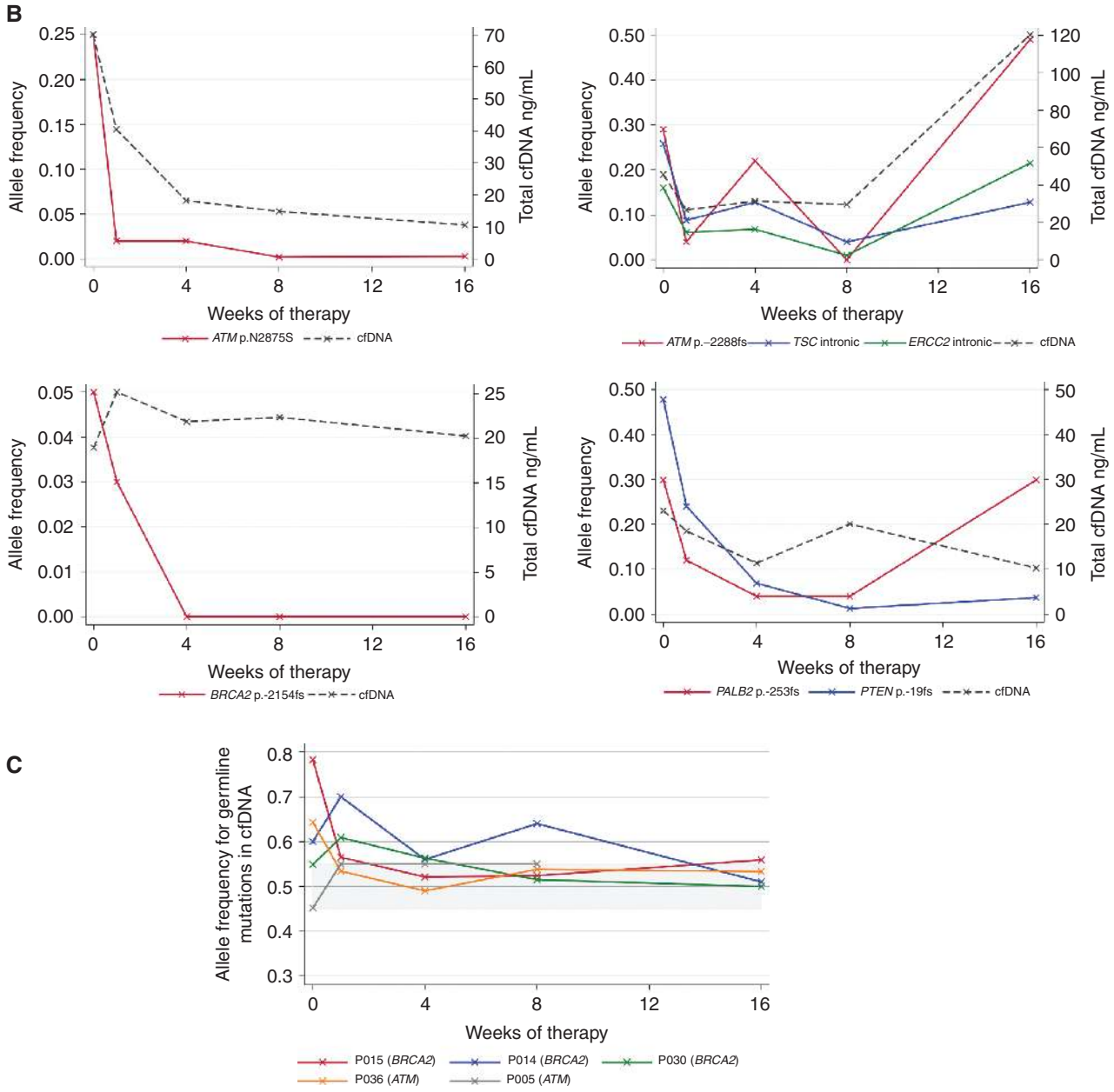

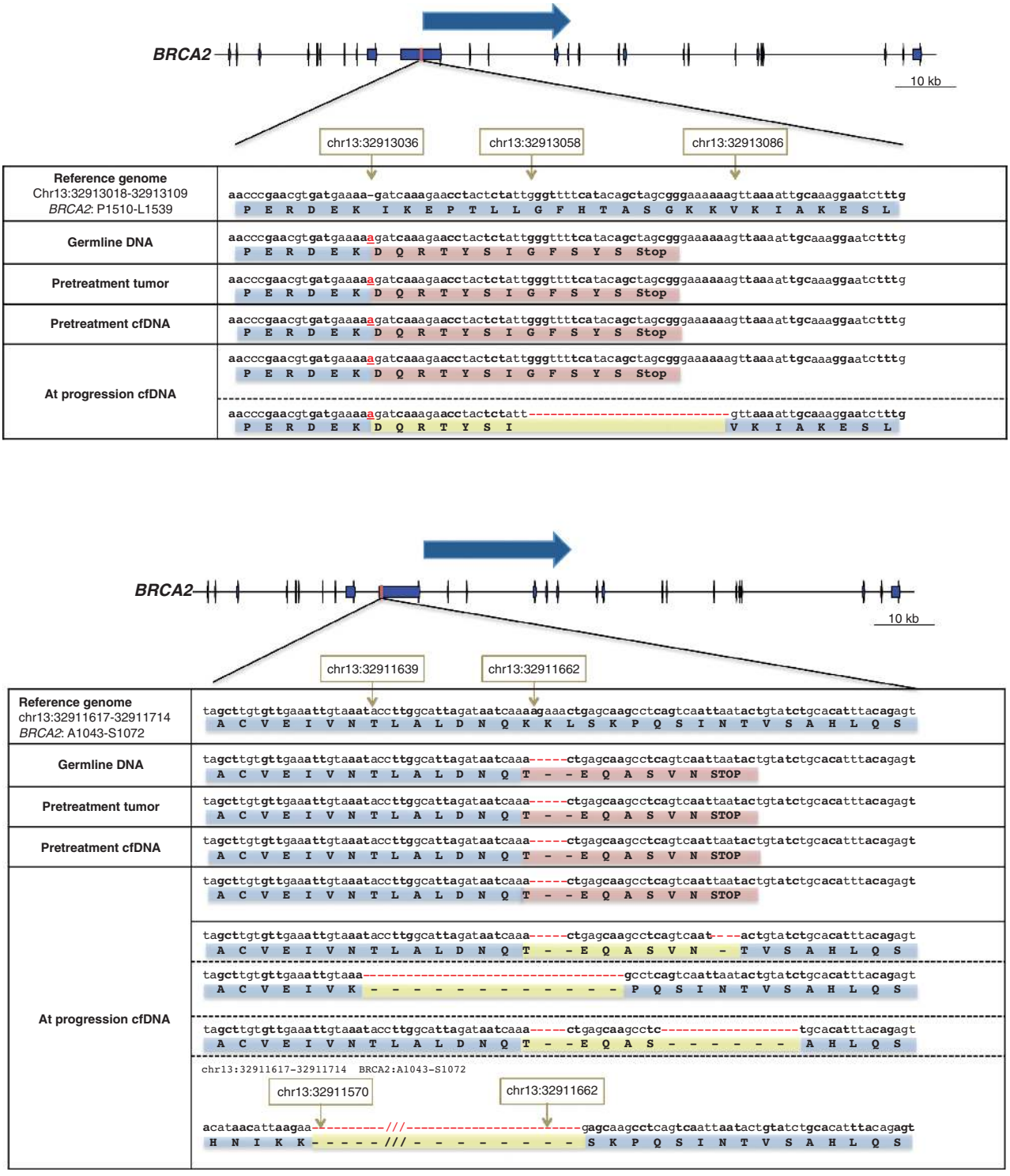

Figure 3. Visual representation of emerging *de novo* mutations at progression that likely result in acquired drug resistance in two patients with germline *BRCA2* mutations. Top, a patient with a germline deleterious *BRCA2* frameshift insertion that was present in both tumor and cfDNA at baseline presents at disease progression with a new frameshift deletion that restores the *BRCA2* reading frame; bottom, a second patient with a germline deleterious *BRCA2* mutation is depicted; at progression cfDNA WES identified multiple clones with different previously undetected mutations all resulting in reversion of the *BRCA2* reading frame to normal.

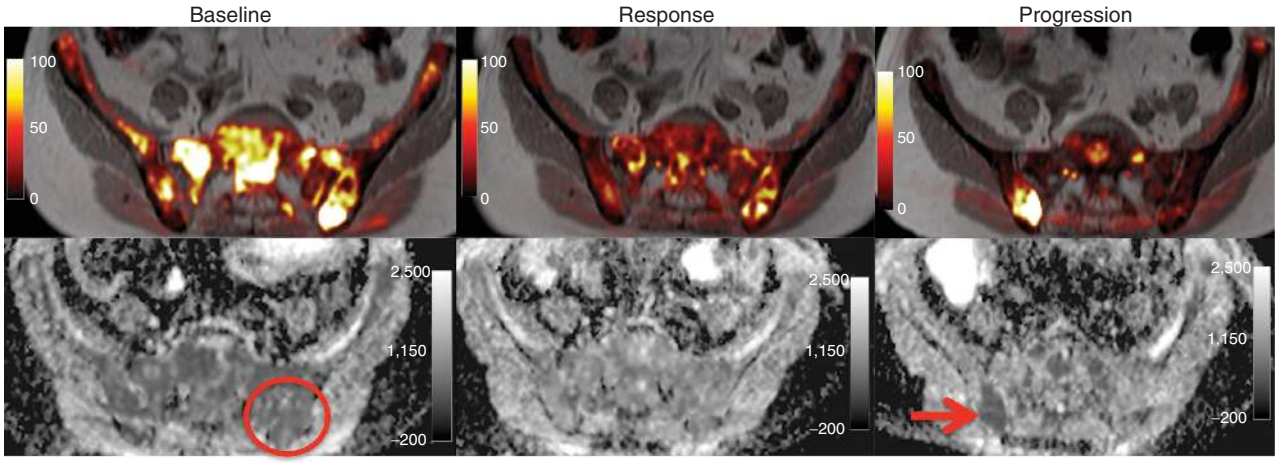

Figure 4. Single-site disease progression after 9 months of response to therapy in the right hemipelvis visualized by diffusion-weighted whole-body MRI. Top, fusion of the T1-weighted imaging and diffusion-weighted imaging; bottom, apparent diffusion coefficient (ADC) maps. Areas of high signal on diffusion-weighted imaging and low ADC values indicate tumor bone marrow infiltration. Left, baseline MRI scan, showing diffuse tumor infiltration in the pelvic bone. The first trial biopsy was taken from the left iliac bone (red circle) and identified a deleterious *BRCA2* mutation with LOH. After 12 weeks of therapy (middle), there was a major response to therapy reported. After 9 months (right), the MRI identified a focal area of tumor relapse in the right iliac bone, which was biopsied (red arrow). Next-generation sequencing of this biopsy confirmed a *de novo* mutation in *BRCA2* restoring the open reading frame.

secondary gene mutations. In some of these multiple resistant subclones emerging in parallel, we observed short regions of nucleotide sequence identity flanking the new deletions. This association with microhomology regions suggests that these might have evolved as a consequence of defective homologous recombination and the utilization of alternative error-prone DNA repair mechanisms.

Finally, in one patient with *HDAC2* biallelic somatic loss in the tumor biopsy, WES demonstrated subclonal divergent evolution and new mutations emerging at progression in *TP53* and *TSC2* (GAP domain), which have been associated with drug resistance (Supplementary Table S1; refs. 20, 21).

Among the remaining patients with plasma cfDNA evaluated at secondary resistance, we did not detect any other such events, although 2 of these patients discontinued the drug due to tolerability issues prior to radiologic progression. No emerging mutations or copy-number changes in *PARP1* or *PARP2* were observed in any of these samples.

DISCUSSION

In this study, we describe the clinical utility of cfDNA analyses as multipurpose biomarkers for treatment with PARP inhibition in metastatic prostate cancer. Critically, our cfDNA analyses detected all somatic HRD-associated mutations identified in tumor biopsies as well as new mutations emerging at disease progression. These new mutations likely represent tumor subclones induced by therapeutic selective pressure driving drug resistance.

The emergence of secondary mutations in *BRCA1/2* germline mutation carriers has been previously described in case reports and small retrospective series of patients with breast or ovarian cancer after PARP inhibition and/or platinum chemotherapy (22–24). Here, we report the first series of patients homogeneously treated within a prospective clinical trial; mutations reverting the reading frame of mutated homologous recombination genes were detected not only in germline *BRCA2* mutation carriers but also, for the first time, in tumors harboring somatic loss of *BRCA2* and *PALB2*. These events were confirmed independently by orthogonal targeted sequencing of cfDNA and/or tumor biopsy DNA.

These multiple genomic events driving resistance emerged in parallel, indicating clonal divergence with functional convergence, restoring homologous recombination repair proficiency. A similar concept has been recently described after exposure to androgen receptor (AR)–targeting agents in prostate cancer, with emergence in parallel of multiple AR aberrations (25–30). Monitoring this subclonal equilibrium between the original clone and resistant clones merits further evaluation, as PARP inhibitor discontinuation and administration of other treatments could potentially restore the dominance of the original clone sensitive to PARP inhibitor or platinum.

Interestingly, in two cases, small tracts of DNA homology flanked all these multiple secondary mutations. These were reminiscent of similar deletions observed in preclinical models restoring the open reading frame of the gene and causing PARP inhibitor resistance, and probably arose from the use of error-prone DNA repair processes that predominate in the absence of functional BRCA2 (31–33).

In the case with the original somatic *PALB2* mutation, the initial clinical response to olaparib, followed by PARPi resistance characterized by the emergence of secondary mutant *PALB2* alleles with microhomology-associated intragenic deletions, is strongly suggestive of the *PALB2* mutation in this patient causing a homologous recombination defect which not only drives the initial PARPi sensitivity phenotype but also the mechanism of resistance that eventually emerges. Although preclinical studies have suggested that PALB2 defects are associated with defective homologous

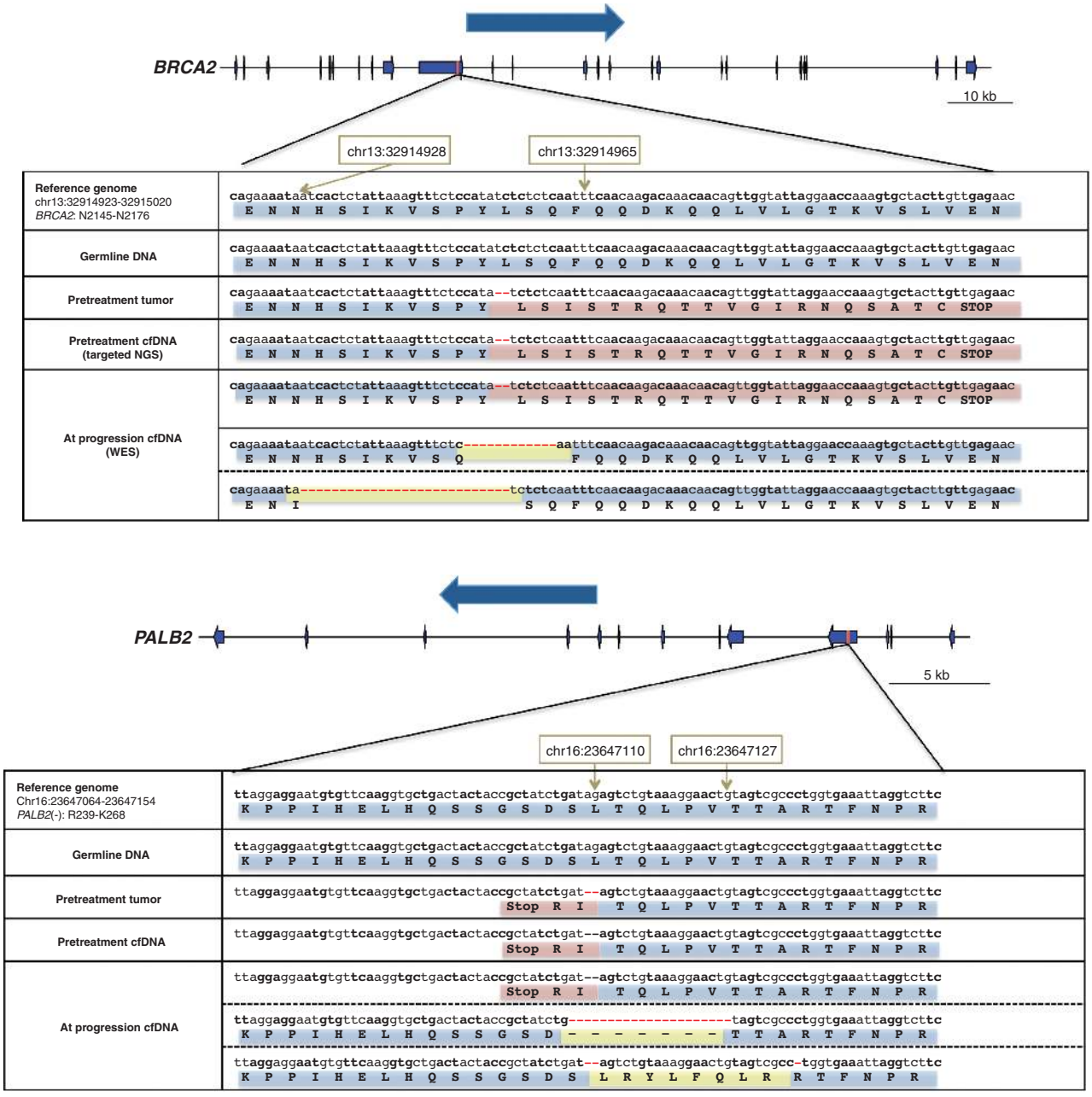

Figure 5. Visual representation of emerging *de novo* mutations at progression that likely result in acquired drug resistance in 2 patients originally presenting somatic frameshift mutations in *BRCA2* (top) and *PALB2* (bottom), respectively, in the pretreatment samples. In both cases, the sample at treatment progression showed two different new deletions resulting in in-frame deletions and restoring the reading frame for *BRCA2* and *PALB2*, respectively. In both cases, these clones were coexisting with the original clone that was present prior to treatment.

recombination, this is to the best of our knowledge the first evidence that the homologous recombination defect caused by a *PALB2* mutation might drive not only drug sensitivity but also resistance.

These data are of major clinical relevance for subsequent treatment strategies for this subset of prostate cancers, and probably also for other cancer types. Platinum chemotherapy also has antitumor activity in *BRCA2*-deficient prostate cancers (34), but our data indicate likely cross-resistance at least for some patients between PARP inhibitors and platinum. Clinical trials of PARP inhibitors and platinum-based chemotherapy in prostate cancer should therefore account for previous exposure to these drugs and the presence of these secondary reversion mutations.

Overall, our data show the potential of serial cfDNA next-generation sequencing to evaluate both temporal and spatial disease heterogeneity. In some cases, cfDNA could monitor the emergence of resistance mechanisms more comprehensively than single-site biopsies. Such analyses may allow us to truly deliver more precise patient care by integrating real-time,

noninvasive, repeated assessment of disease biology. Our study also shows that simple, inexpensive, cfDNA quantification, and tumor mutation allele frequency analyses, have clinical utility as a response biomarker to guide early treatment switch decisions in the presence of ineffective therapies. Although further validation studies are needed, these findings may be of huge importance, as earlier discontinuation of therapy for futility can spare patients the toxicity of ineffective overtreatment, allowing these men to receive alternative therapy and decreasing treatment health economic costs to fund these cfDNA studies.

A limitation of our study is that we did not collect samples between week 16 of therapy and cancer progression, which in some cases meant over a year of olaparib therapy. Therefore, we were unable to determine precisely when these restoring resistance mutations emerged; this has clinical relevance as these may appear before disease progression detection by established methods and allow earlier treatment changes. In the ongoing TOPARP-B trial, which is further evaluating responses to olaparib in patients with metastatic prostate cancer, preselected based on DNA repair aberrations, monthly samples are being collected to address this. Furthermore, our assays were limited to exon sequencing, so it remains possible that some of these tumors had alternative undetected resistance mechanisms.

In conclusion, we provide strong evidence that serial cfDNA analyses are a powerful test for guiding prostate cancer care allowing disease molecular stratification, response assessment, and the study of emerging resistant clones. Critically, we report previously undetectable divergent emerging subclones in cfDNA only at disease progression due to treatment-selective pressures, with multiple reversion genomic events restoring the DNA repair gene function, all causing acquired resistance through convergent mechanisms. Directing patient treatment through the early detection of emerging resistant tumor clones in cfDNA, either by adding other treatments or by switching therapy contingent on which clone is dominant, is envisioned. This could have a major impact on the treatment and outcome of not only prostate cancer but also other malignancies.

METHODS

Study Population

All samples were collected prospectively as part of the TOPARP-A clinical trial (CRUK/11/029; NCT01682772). Patients provided written informed consent prior to trial participation. Full details of trial design, eligibility criteria, and response to treatment have been reported previously (10). The study of cfDNA as response and resistance biomarker was included as an exploratory endpoint of the study.

cfDNA Extraction and Quantification

Thirty milliliters of blood was collected in CTP tubes from each patient at prespecified time points: at baseline and after 1, 4, 8, and 16 weeks of therapy, and at disease progression when possible. Circulating free DNA was extracted from 4 to 8 mL of plasma using the QIAsymphony (Qiagen) and the Circulating DNA Kit (Qiagen) and quantified by Quant-iT High Sensitivity Picogreen Kit (Invitrogen).

Targeted cfDNA Sequencing

Targeted next-generation sequencing was performed as described previously (10). Libraries were constructed from 40 ng of cfDNA using a customized GeneRead DNAseq Mix-n-Match v2 panel (Qiagen) and sequenced on the MiSeq Sequencer (Illumina). The somatic variant calls were manually inspected in the Integrative Genomics Viewer (Broad Institute, Cambridge, MA).

Whole-Exome cfDNA Sequencing

WES was performed using Kapa Hyper Plus Library Prep Kits and the Agilent SureSelectXT V6 target enrichment system. Paired-end sequencing was performed using the NextSeq 500 (2 × 150 cycles; Illumina). FASTQ files were generated from the sequencer's output using Illumina bcl2fastq2 software (v.2.17.1.14, Illumina) with the default chastity filter to select sequence reads for subsequent analysis. All sequencing reads were aligned to the human genome reference sequence (GRCh37) using the BWA (v. 0.7.12) MEM algorithm, with indels being realigned using the Stampy (v.1.0.28) package. Picard tools (v.2.1.0) were used to remove PCR duplicates and to calculate sequencing metrics for quality control check. The Genome Analysis Toolkit (GATK, v. 3.5-0) was then applied to realign local indels, recalibrate base scores, and identify point mutations and small insertions and deletions. Somatic point mutations and indels were called using MuTect2 by comparing tumor/plasma DNA to germline control, and copy-number estimation was obtained through modified ASCAT2 package.

Statistical Analyses

rPFS was defined as the time from trial entry to progression (RECIST 1.1, bone scan-PCWG2; refs. 35, 36) or death. OS was defined as the time from trial entry to death. Response was defined in the trial protocol as either response by RECIST 1.1, PSA decline of ≥50%, and/or conversion of CTC from baseline ≥5 cells to <5 cells/7.5 mL on treatment, requiring a confirmatory assessment at least 4 weeks later. Mann–Whitney and Fisher exact tests were used to assess the association of continuous and categorical variables with response. Kaplan–Meier curves are presented for time-to-event endpoints. The prognostic significance of changes in cfDNA at week 4 and week 8 from baseline were explored using landmark analyses. Patients experiencing rPFS and/or OS events before the landmark time were excluded. HRs were estimated utilizing Cox regression univariate and multivariable models; 95% CIs are provided. In the absence of a validated cutoff, log fold change, 30% and 50% declines in cfDNA were evaluated. The proportional hazards assumption of the Cox model was tested using Schoenfeld residuals. On the basis of the exploratory nature of these analyses, Bonferroni adjustment of P values was not pursued but a P value <0.01 was predefined as significant to account for multiple testing. Statistical analyses were conducted using STATA13 (StataCorp LP) on a data snapshot taken on May 24, 2016, when 49 of 50 patients had discontinued the trial.

Disclosure of Potential Conflicts of Interest

S. Sandhu has received speakers bureau honoraria from Bristol-Myers Squibb and Merck. J.S. de Bono has received speakers bureau honoraria from AstraZeneca and is a consultant/advisory board member for the same. No potential conflicts of interest were disclosed by the other authors.

Authors' Contributions

Conception and design: J. Goodall, J. Mateo, S. Sandhu, E. Hall, S. Carreira, J.S. de Bono

Development of methodology: J. Goodall, W. Yuan, S. Miranda, S. Sandhu, S. Carreira, J.S. de Bono

Acquisition of data (provided animals, acquired and managed patients, provided facilities, etc.): J. Goodall, J. Mateo, R. Perez-Lopez, D.R. Robinson, S. Sandhu, G. Fowler, B. Ebbs, P. Flohr, M. Atkin, M. Crespo, P. Rescigno, Z. Zafeiriou, N. Tunariu, D. Bianchini, A. Gillman, E. Hall, A.M. Chinnaiyan, S. Carreira, J.S. de Bono

Analysis and interpretation of data (e.g., statistical analysis, biostatistics, computational analysis): J. Goodall, J. Mateo, W. Yuan, H. Mossop, N. Porta, D. Dolling, D.R. Robinson, S. Sandhu, G. Seed,

M. Clarke, I. Figueiredo, P. Rescigno, N. Tunariu, C.J. Lord, E. Hall, A.M. Chinnaiyan, S. Carreira, J.S. de Bono
Writing, review, and/or revision of the manuscript: J. Goodall, J. Mateo, W. Yuan, H. Mossop, N. Porta, S. Miranda, R. Perez-Lopez, D. Dolling, S. Sandhu, G. Fowler, B. Ebbs, P. Flohr, G. Seed, G. Boysen, R. Riisnaes, S. Sumanasuriya, P. Rescigno, A. Sharp, D. Bianchini, A. Gillman, C.J. Lord, E. Hall, S. Carreira, J.S. de Bono
Administrative, technical, or material support (i.e., reporting or organizing data, constructing databases): J. Goodall, J. Mateo, R. Perez-Lopez, G. Fowler, B. Ebbs, P. Flohr, D. Nava Rodrigues, C. Bertan, S. Carreira, J.S. de Bono
Study supervision: J. Mateo, E. Hall, S. Carreira, J.S. de Bono
Other (sequencing): C. Bertan
Other (member of trial management, oversight of trial conduct, and sample collection): A. Gillman

Grant Support

We would like to acknowledge funding support from Movember (Movember/PCUKCEO13-2-002); Prostate Cancer Foundation (PCF grant 20131017); Prostate Cancer UK (PCUK PG12-49); a Stand Up To Cancer–Prostate Cancer Foundation Prostate Dream Team Translational Cancer Research Grant (SU2C-AACR-DT0712; PCF grants 20131017 and 20131017-1); Cancer Research UK (Centre Programme grant); Experimental Cancer Medicine Centre grant funding from Cancer Research UK and the Department of Health; and Biomedical Research Centre funding to the Royal Marsden (ECMC CRM064X). Stand Up To Cancer is a program of the Entertainment Industry Foundation administered by the American Association for Cancer Research. TOPARP is an investigator-initiated study supported by Cancer Research UK (grants C12540/A12829, C12540/A13230, C1491/A9895, and C1491/A15955) and conducted with support from the Investigator-Sponsored Study Collaboration between AstraZeneca and the National Institute for Health Research Cancer Research Network. J. Mateo was supported by a Prostate Cancer Foundation (PCF) Young Investigator Award (PCF-16-YOUN11) and a Prostate Cancer UK-Medical Research Council Fellowship (MR/M003272/1). S. Sandhu was supported by the Prostate Cancer Foundation of Australia. G. Seed was supported by a Prostate Cancer UK PhD Studentship (TLD-S15-006). A. Sharp was supported by a Medical Research Council Fellowship (MR/M018618/1).

Received March 14, 2017; revised April 15, 2017; accepted April 26, 2017; published OnlineFirst April 27, 2017.

REFERENCES

1. Grasso CS, Wu Y-M, Robinson DR, Cao X, Dhanasekaran SM, Khan AP, et al. The mutational landscape of lethal castration-resistant prostate cancer. Nature 2012;487:239–43.
2. Beltran H, Yelensky R, Frampton GM, Park K, Downing SR, MacDonald TY, et al. Targeted next-generation sequencing of advanced prostate cancer identifies potential therapeutic targets and disease heterogeneity. Eur Urol 2013;63:920–6.
3. Abeshouse A, Ahn J, Akbani R, Ally A, Amin S, Andry CD, et al. The molecular taxonomy of primary prostate cancer. Cell 2015;163:1011–25.
4. Robinson D, Van Allen EM, Wu Y-M, Schultz N, Lonigro RJ, Mosquera J-M, et al. Integrative clinical genomics of advanced prostate cancer. Cell 2015;161:1215–28.
5. Gundem G, Van Loo P, Kremeyer B, Alexandrov LB, Tubio JMC, Papaemmanuil E, et al. The evolutionary history of lethal metastatic prostate cancer. Nature 2015;520:353–7.
6. Boutros PC, Fraser M, Harding NJ, de Borja R, Trudel D, Lalonde E, et al. Spatial genomic heterogeneity within localized, multifocal prostate cancer. Nat Genet 2015;47:736–45.
7. Kumar A, Coleman I, Morrissey C, Zhang X, True LD, Gulati R, et al. Substantial interindividual and limited intraindividual genomic diversity among tumors from men with metastatic prostate cancer. Nat Med 2016;22:369–78.
8. Castro E, Goh C, Olmos D, Saunders E, Leongamornlert D, Tymrakiewicz M, et al. Germline BRCA mutations are associated with higher risk of nodal involvement, distant metastasis, and poor survival outcomes in prostate cancer. J Clin Oncol 2013;31:1748–57.
9. Pritchard CC, Mateo J, Walsh MF, De Sarkar N, Abida W, Beltran H, et al. Inherited DNA-repair gene mutations in men with metastatic prostate cancer. N Engl J Med 2016;375:443–53.
10. Mateo J, Carreira S, Sandhu S, Miranda S, Mossop H, Perez-Lopez R, et al. DNA-repair defects and olaparib in metastatic prostate cancer. N Eng J Med 2015;373:1697–708.
11. de Bono J, Ramanathan RK, Mina L, Chugh R, Glaspy J, Rafii S, et al. Phase I, dose-escalation, 2-part trial of Poly(ADP-Ribose) polymerase inhibitor talazoparib in patients with advanced germline BRCA1/2 mutations and selected sporadic cancers. Cancer Discov 2017 Feb 27. [Epub ahead of print].
12. Sandhu SK, Schelman WR, Wilding G, Moreno V, Baird RD, Miranda S, et al. The poly(ADP-ribose) polymerase inhibitor niraparib (MK4827) in BRCA mutation carriers and patients with sporadic cancer: a phase 1 dose-escalation trial. Lancet Oncol 2013;2045:1–11.
13. Fong PCP, Boss DDS, Yap TA, Tutt A, Wu P, Mergui-Roelvink M, et al. Inhibition of poly (ADP-ribose) polymerase in tumors from BRCA mutation carriers. N Engl J Med 2009;361:123–34.
14. Perez-Lopez R, Mateo J, Mossop H, Blackledge MD, Collins DJ, Rata M, et al. Diffusion-weighted imaging as a treatment response biomarker for evaluating bone metastases in prostate cancer: a pilot study. Radiology 2017;283:168–77.
15. Frenel J-S, Carreira S, Goodall J, Roda Perez D, Perez Lopez R, Tunariu N, et al. Serial next generation sequencing of circulating cell free DNA evaluating tumour clone response to molecularly targeted drug administration. Clin Cancer Res 2015;15:4586–96.
16. Maheswaran S, Sequist LV, Nagrath S, Ulkus L, Brannigan B, Collura CV, et al. Detection of mutations in EGFR in circulating lung-cancer cells. New Eng J Med 2008;359:366–77.
17. Scher HI, Heller G, Molina A, Attard G, Danila DC, Jia X, et al. Circulating tumor cell biomarker panel as an individual-level surrogate for survival in metastatic castration-resistant prostate cancer. J Clin Oncol 2015;33:1348–55.
18. Schwarzenbach H, Alix-Panabières C, Müller I, Letang N, Vendrell J-P, Rebillard X, et al. Cell-free tumor DNA in blood plasma as a marker for circulating tumor cells in prostate cancer. Clin Cancer Res 2009;15:1032–8.
19. Thierry AR, Mouliere F, El Messaoudi S, Mollevi C, Lopez-Crapez E, Rolet F, et al. Clinical validation of the detection of KRAS and BRAF mutations from circulating tumor DNA. Nat Med 2014;20:430–5.
20. Cardnell RJ, Feng Y, Mukherjee S, Diao L, Tong P, Stewart CA, et al. Activation of the PI3K/mTOR pathway following PARP inhibition in small cell lung cancer. PLoS One 2016;11:e0152584.
21. Aas T, Børresen A-L, Geisler S, Smith-Sørensen B, Johnsen H, Varhaug JE, et al. Specific P53 mutations are associated with de novo resistance to doxorubicin in breast cancer patients. Nat Med 1996;2:811–4.
22. Norquist B, Wurz KA, Pennil CC, Garcia R, Gross J, Sakai W, et al. Secondary somatic mutations restoring BRCA1/2 predict chemotherapy resistance in hereditary ovarian carcinomas. J Clin Oncol 2011;29:3008–15.
23. Afghahi A, Timms KM, Vinayak S, Jensen KC, Kurian AW, Carlson RW, et al. Tumor BRCA1 reversion mutation arising during neoadjuvant platinum-based chemotherapy in triple-negative breast cancer is associated with therapy resistance. Clin Cancer Res 2017 Jan 13. [Epub ahead of print].
24. Barber LJ, Sandhu S, Chen L, Campbell J, Kozarewa I, Fenwick K, et al. Secondary mutations in BRCA2 associated with clinical resistance to a PARP inhibitor. J Pathol 2013;229:422–9.
25. Antonarakis ES, Lu C, Wang H, Luber B, Nakazawa M, Roeser JC, et al. AR-V7 and resistance to enzalutamide and abiraterone in prostate cancer. New Eng J Med 2014;371:1028–38.
26. Carreira S, Romanel A, Goodall J, Grist E, Ferraldeschi R, Miranda S, et al. Tumor clone dynamics in lethal prostate cancer. Sci Transl Med 2014;6:254ra125.

27. Romanel A, Tandefelt DG, Conteduca V, Jayaram A, Casiraghi N, Wetterskog D, et al. Plasma AR and abiraterone-resistant prostate cancer. Sci Transl Med 2015;7:312re10.
28. Wyatt AW, Azad AA, Volik S V, Annala M, Beja K, McConeghy B, et al. Genomic Alterations in Cell-Free DNA and enzalutamide resistance in castration-resistant prostate cancer. JAMA Oncol 2016;2:1598–606.
29. Henzler C, Li Y, Yang R, McBride T, Ho Y, Sprenger C, et al. Truncation and constitutive activation of the androgen receptor by diverse genomic rearrangements in prostate cancer. Nat Commun 2016;7:13668.
30. De Laere B, van Dam P-J, Whitington T, Mayrhofer M, Diaz EH, Van den Eynden G, et al. Comprehensive profiling of the androgen receptor in liquid biopsies from castration-resistant prostate cancer reveals novel Intra-AR structural variation and splice variant expression patterns. Eur Urol 2017 Jan 16. [Epub ahead of print].
31. Edwards SL, Brough R, Lord CJ, Natrajan R, Vatcheva R, Levine DA, et al. Resistance to therapy caused by intragenic deletion in BRCA2. Nature 2008;451:1111–5.
32. Tutt A, Bertwistle D, Valentine J, Gabriel A, Swift S, Ross G, et al. Mutation in Brca2 stimulates error-prone homology-directed repair of DNA double-strand breaks occurring between repeated sequences. EMBO J 2001;20:4704–16.
33. Moynahan ME, Pierce AJ, Jasin M. BRCA2 is required for homology-directed repair of chromosomal breaks. Mol Cell 2001;7:263–72.
34. Cheng HH, Pritchard CC, Boyd T, Nelson PS, Montgomery B. Biallelic Inactivation of BRCA2 in platinum-sensitive metastatic castration-resistant prostate cancer. Eur Urol 2016;69:992–5.
35. Scher HI, Halabi S, Tannock I, Morris M, Sternberg CN, Carducci MA, et al. Design and end points of clinical trials for patients with progressive prostate cancer and castrate levels of testosterone: recommendations of the prostate cancer clinical trials working group. J Clin Oncol 2008;26:1148–59.
36. Eisenhauer EA, Therasse P, Bogaerts J, Schwartz LH, Sargent D, Ford R, et al. New response evaluation criteria in solid tumours: Revised RECIST guideline (version 1.1). Eur J Cancer 2009;45:228–47.